HEDL-SA-2014

CONF-800231--1

MASTER

ULTRASONIC OFF-NORMAL IMAGING TECHNIQUES

FOR

UNDER-SODIUM VIEWING

T. E. Michaels and J. E. Horn

December 6, 1979

THIRD INTERNATIONAL CONFERENCE ON NONDESTRUCTIVE EVALUATION IN THE NUCLEAR INDUSTRY

SALT LAKE CITY, UT 2/11-13,80

HANFORD ENGINEERING DEVELOPMENT LABORATORY
Operated by Westinghouse Hanford Company, a subsidiary of Westinghouse Electric Corporation, under the Department of Energy Contract No. EY-76-C-14-2170

DISCLAIMER

DISCLAIMER

Portions of this document may be illegible in electronic image products. Images are produced from the best available original document.

ULTRASONIC OFF-NORMAL IMAGING TECHNIQUES

FOR

UNDER SODIUM VIEWING

T. E. Michaels and J. E. Horn

ABSTRACT

Advanced imaging methods have been evaluated for the purpose of constructing images of objects from ultrasonic data. Feasibility of imaging surfaces which are off-normal to the sound beam has been established. Laboratory results are presented which show a complete image of a typical core component. Using the previous system developed for under sodium viewing (USV), only normal surfaces of this object could be imaged. Using advanced methods, surfaces up to 60 degrees off-normal have been imaged. Details of equipment and procedures used for this image construction are described. Additional work on high temperature transducers, electronics, and signal analysis is required in order to adapt the off-normal viewing process described here to an eventual USV application.

I. INTRODUCTION

Under Sodium Viewing (USV) is the process of viewing objects immersed in optically opaque liquid sodium. At HEDL, this viewing is accomplished by using ultrasonic techniques. Specifically, methods and equipment have been developed for scanning an array of ultrasonic transducers above objects immersed in liquid sodium, and for forming images of these objects from the ultrasonic energy that is reflected and scattered from the objects. In earlier reported work, simple pulse-echo ultrasonic methods were used, and only surfaces normal to the sound beam could be successfully imaged.[1] Surfaces tilted off-normal did not return distinct enough echoes to permit direct image formation. This was because echoes from off-normal surfaces were of very small amplitude and of unpredictable pulse shape.

Off-normal imaging capability is desired in order to increase the range and flexibility of the USV system. With the existing system, objects to be viewed must be directly under the transducer sweep arm. Hence, the viewing angle for the sweep arm is limited to the cylinder formed vertically below the sweep arm during its rotation. Further, within this cylinder only surfaces normal to the sound beam; i.e., normal to the axis of this cylinder, can be imaged. However, with off-normal capabilities, viewing could hopefully be extended outside this cylinder, and additionally, more complete images could be made of objects within this cylinder.

II. LABORATORY INSTRUMENTATION SYSTEM

The laboratory instrumentation system used for this study consisted of a scanner, ultrasonic pulsers and receivers, electronics for waveform digitizing, a central computer and a graphics display. A block diagram of this system is shown in Figure 1 and the system is shown in Figure 2. This system is completely programmable and controlled by the central computer. All interfacing, with exception of the waveform digitizer, was done using a specially designed hardware interface. The three mechanical scanner motions

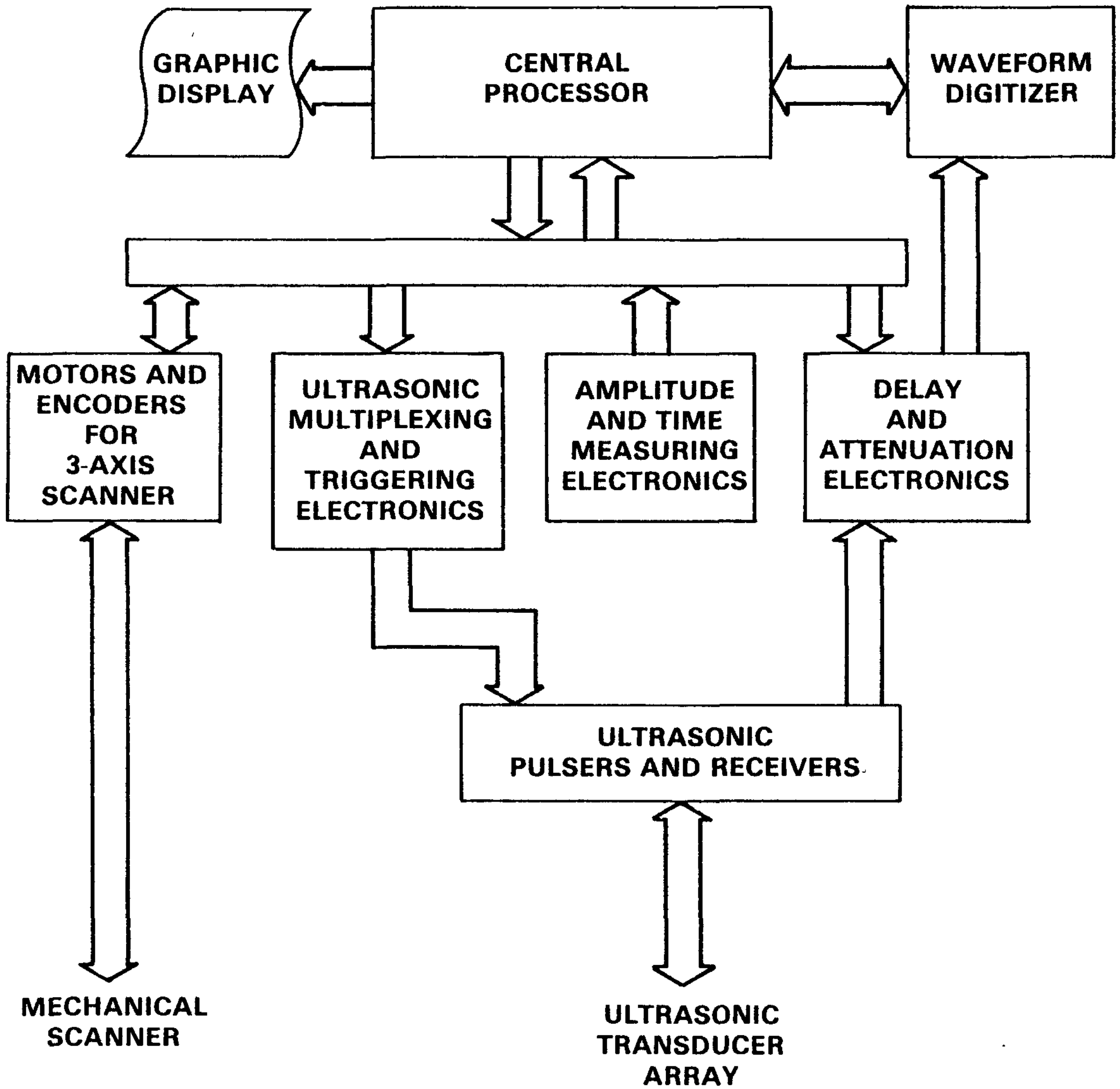

FIGURE 1. LABORATORY SYSTEM FOR OFF-NORMAL IMAGING STUDIES

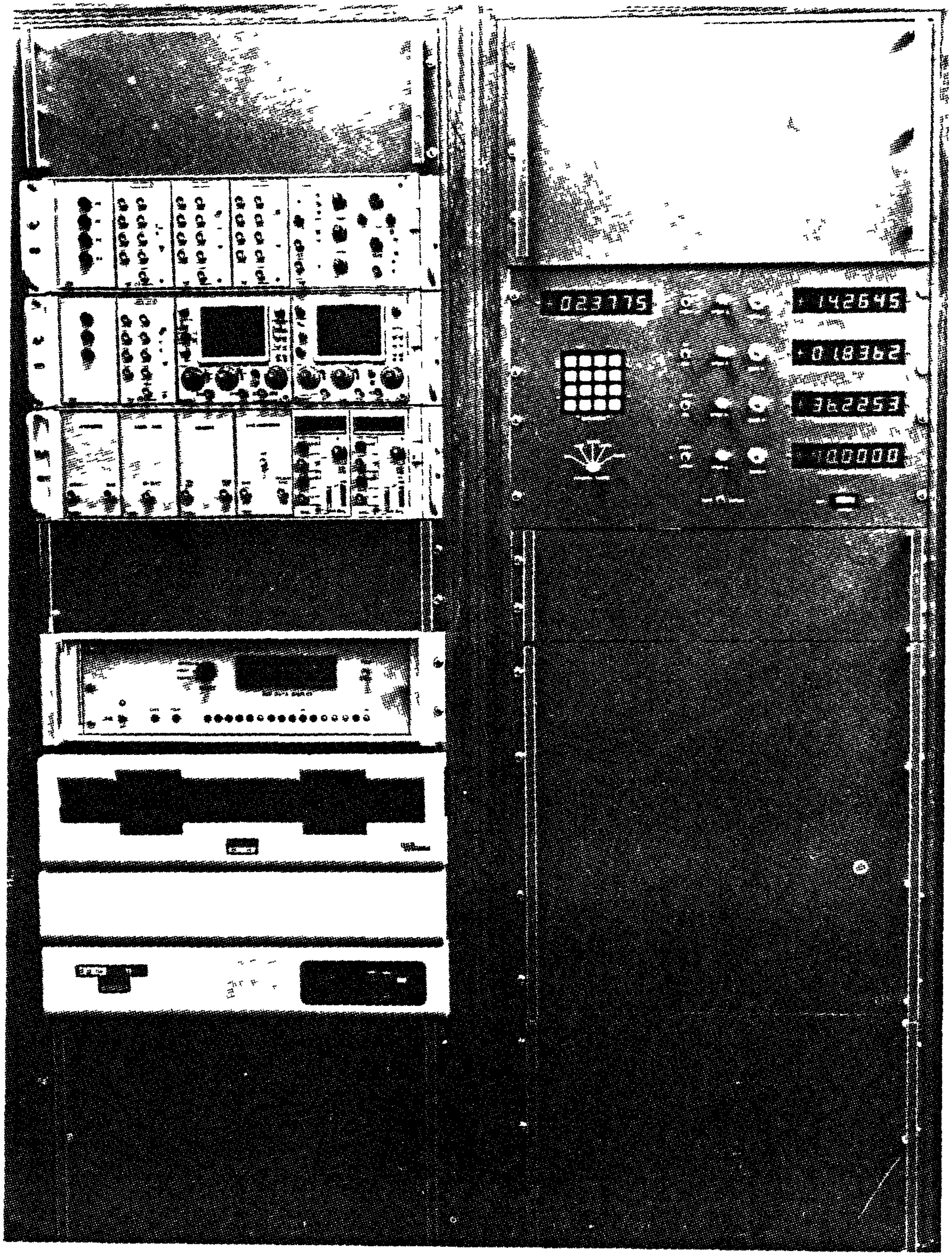

FIGURE 2. UNDER SODIUM VIEWING INSTRUMENTATION SYSTEM

were controlled to within ± 0.0005 inch (0.013 mm) absolute position for each axis. The ultrasonic system consisted of pulsers and receivers for several transducers, multiplexing electronics to permit channel selection (one transducer per channel), electronics for controlling delay and attenuation of the ultrasonic signal, and circuitry for measuring peak amplitude and time from transmit of return echoes. Ultrasonic waveforms were also input to a waveform digitizer (transient digitizer) to permit digital input to the central processor. The central processor was used to control the scan, to try various algorithms for image formation, and to construct these images on the graphics terminal.

III. OFF-NORMAL FLAT PLATE OBSERVATIONS

Initial experiments were performed to determine if sufficient energy is received from off-normal objects to permit imaging. This was accomplished by studying echoes scattered back to the transducer from a flat plate inclined at 0°, 30°, 45°, and 60° from horizontal. At 0° the scattered energy was the directly reflected component, while at the other angles only diffuse scattered energy was received. The plate was polished aluminum (∿ 3/8" thickness), and the transducer was 5 Mhz, medium bandwidth, with a 1- to 2-inch focal zone. For this experiment and others to follow, the transducer-to-object distance was approximately 5 inches.

Waveforms received from the flat plate are shown in Figure 3. At each angle three waveforms were stored for different scanner coordinates as given in Table I. These scanner positions were in an X-Y plane above the flat plate, and the angle of inclination was then the angle between the Z axis and the plate normal. Therefore, for the 0° case, there is no difference in transit time between the plate and the transducer for these X-Y plane scanner motions. Correspondingly, the three waveform traces show no transit time differences. The first signal is the surface echo and the weak signal about 3 μsec behind the surface echo is the first internal reflection from the back of the flat plate. Input attenuation for the system was set at 70 db for each of the 0° waveforms.

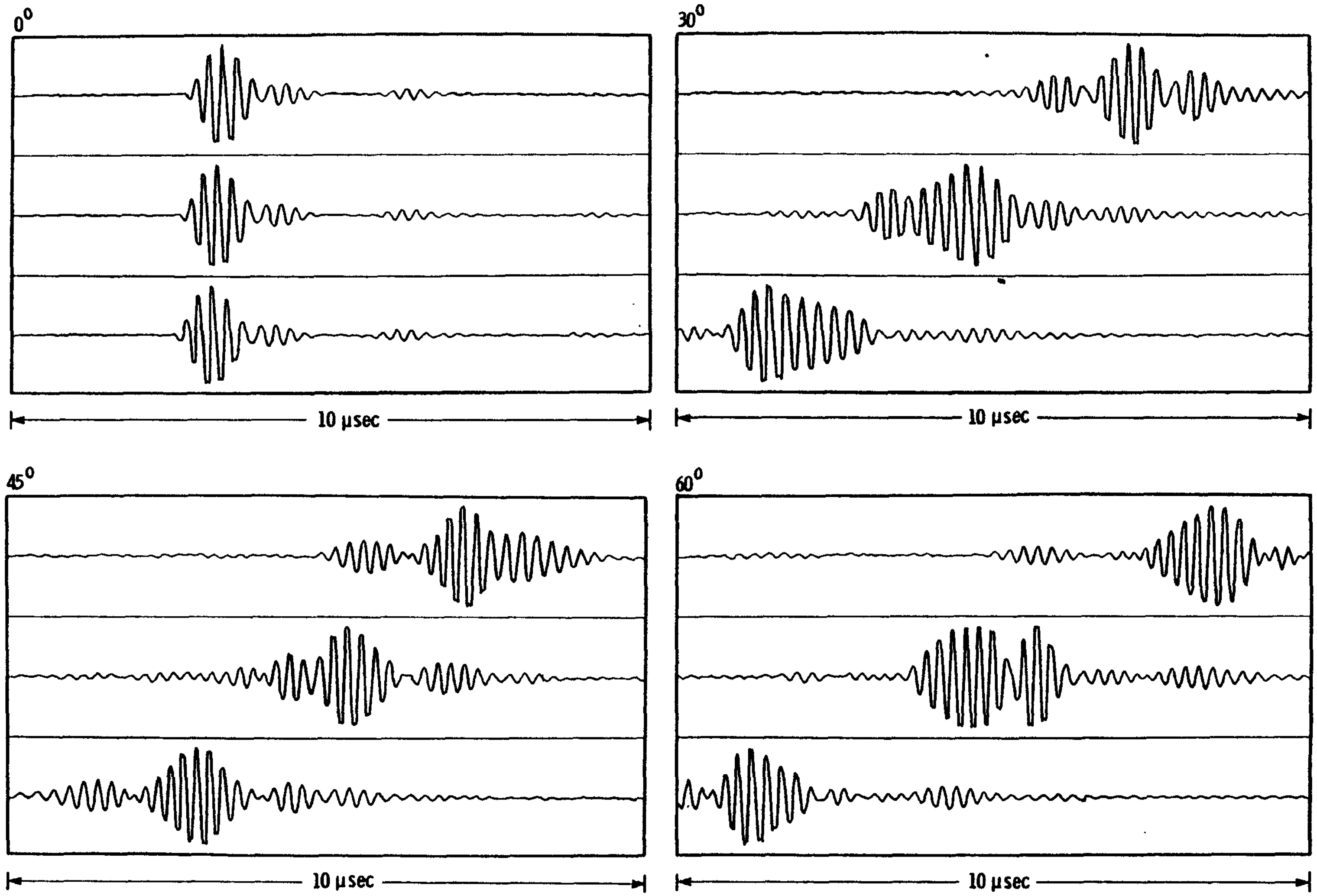

FIGURE 3. ULTRASONIC WAVEFORMS FROM FLAT PLATE TESTS

TABLE I

SUMMARY OF TEST PARAMETERS AND COORDINATES FOR
INCLINED FLAT PLATE EXPERIMENT SHOWN IN FIGURE 3

TEST NAME	NOMINAL ANGLE (DEGREES)	RELATIVE GAIN (DB)	COORDINATES X (INCHES)*	COORDINATES Z (INCHES)*
USVDAT.008	0	0	0.000	3.1930
			0.100	3.1953
			0.200	3.1977
USVDAT.005	30	46	0.000	3.3137
			0.150	3.2349
			0.300	3.1496
USVDAT.006	45	55	0.000	3.3125
			0.060	3.2570
			0.120	3.1877
USVDAT.010	60	54	0.000	3.3492
			0.070	3.2444
			0.140	3.1386

* X = Actual Scanner Position

Z = Calculated Distance from Transducer to Flat Plate Surface

Observations from flat plate experiments may be summarized as follows:

1. There is a shift in transit time corresponding to X-Y scanner motions for the centroid of the received pulse scattered from an off-normal surface.

2. The received signal amplitude is much weaker than the directly reflected component for the 0° case.

3. Scattered energy from off-normal surfaces is not a monotonic function of angle of inclination.

4. Pulse shape of the scattered energy varies substantially as a function local position on the inclined surface.

These observations provided guidance to us in choosing algorithms for processing images from off-normal surfaces. It is obvious why existing USV equipment with fixed energy trigger levels would not be appropriate for off-normal imaging. Further, algorithms based upon absolute pulse shape would not accommodate variations observed in waveforms from inclined surfaces. Thus, we sought an algorithm which could track the centroid of the received scattered energy as a function of transit time. Along with known scanner coordinates, this would provide sufficient data for image formation.

IV. IMAGE ALGORITHM DEVELOPMENT

Several algorithms were contemplated for finding the centroid of the received waveform. These included cross-correlation of a specific point waveform to an average waveform, and percent accumulated pulse energy received at each position. These methods are discussed in the following text.

The cross-correlation method would involve keeping a running average of the background pulse shape (or pulse envelope), and then performing a waveform cross-correlation between this background waveform and the local waveform at each position. The peak in the cross-correlation signal should correspond to best overlap between these waveforms, and the time offset of overlap would directly yield transit time (actually relative transit time), which is the desired quantity required for imaging. This method should work very well as it would automatically compensate for pulse shape difference, and the peak for correlation would be insensitive to level differences. However, it would be expensive in computer time because one algorithm would be required to formulate the average background signal in addition to the final cross-correlation step.

The accumulated pulse energy approach involves integrating the pulse energy as a function of transit time for each received waveform. Transit time can then be found for the half energy value, or any energy value that supports good imaging results. This algorithm was tried and gave such good results that further work with the cross-correlation scheme was postponed. The remainder of this report describes this accumulated energy algorithm and presents imaging results.

Recall for each slope of the flat plate experiment, ultrasonic waveforms were digitized and stored at three different positions along the plate. Thus, actual slopes can be compared to those computed from time change data of the received signals. With the accumulated energy method, we calculated time-from-transmit by finding where the center of energy occurs for the received waveform.

$$n_t = n_t : \sum_{i=1}^{n_t} w_i^2 = \frac{1}{2} \sum_{i=1}^{N} w_i^2 \qquad (1)$$

$$t = t_o + n_t \cdot sf \tag{2}$$

w_i = i^{th} sample of ultrasonic waveform

N = total number of sample points

$\sum_{i=1}^{N} w_i^2$ = total energy

t_o = delay from transmit

sf = time scale factor ($N \cdot sf$ = width of time window)

n_f = sample at which the center of energy occurs

t = calculated time-from-transmit

Distance from the transducer to the plate can now be calculated:

$$d = 1/2 \; v_c t \tag{3}$$

v_c = couplant acoustic velocity

At three horizontal positions for each slope, the transducer-plate distance is now known. The best straight line can be drawn through these points to calculate the slope, and hence the inclination angle. This was done for all four slopes, with results presented in Table 2.

Error values here are judged very good since the actual plate angle was only known to $\pm$ 3° for these experiments.

TABLE II

COMPARISON OF ACTUAL ANGLES AND ANGLES COMPUTED FROM ULTRASONIC DATA FROM INCLINED FLAT PLATE EXPERIMENTS

ACTUAL ANGLE (DEGREES)	CALCULATED ANGLE (DEGREES)	ERROR (PERCENT)
0	1.34	--
30	28.7	4.3
45	46.1	2.4
60	56.4	6.0

A. IMAGING RESULTS

The techniques described above were applied to the imaging of a complex object--a simulated handling socket. This object and the setup are shown in Figure 4. The resulting ultrasonic image is shown in Figure 5 alongside a photograph taken at the same perspective. This image is very promising, as much of the dimensional detail of the object is apparent in the image. Note that both flat and curved surfaces were properly imaged. The background for this ultrasonic image is the plate which supports the handling socket shown in Figure 4.

This image was made in the following manner. A two dimensional scan was performed by moving the transducer in a horizontal plane above the object. Ultrasonic waveforms were digitized at discrete points in this plane. At each scan grid point, transducer-to-object distances were calculated as outlined in equations 1-3. These distances added a third dimension describing the exposed surface of the object. These coordinates are stored in the computer and can be displayed in many different ways, such as the image in Figure 5.

One requirement for successful imaging is that the system used should be able to handle the wide range of signal levels that are received from off-normal surfaces. Figure 6 shows spatial and energy cross-sections from the scan of the handling socket. Notice that the quality of the spatial information is independent of signal level.

Another useful display of scan results is the shadow from one object cast on other components. Such a method is valuable for approximately locating objects and to permit mechanism alignment for more precise imaging scans. Figure 7 shows the shadow cast by the handling socket on the supporting plate.

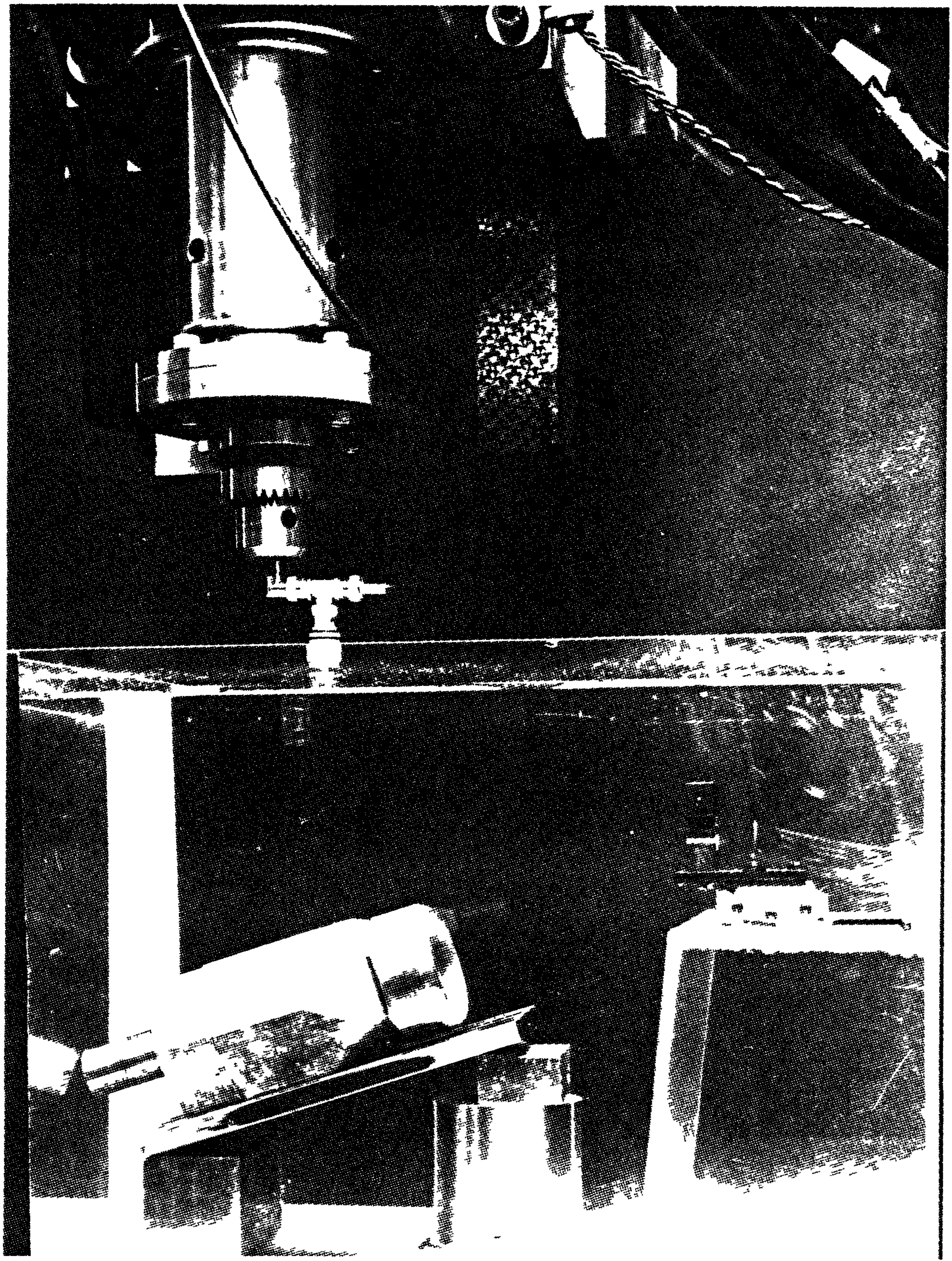

FIGURE 4. SETUP FOR ULTRASONIC IMAGING OF A SIMULATED HANDLING SOCKET

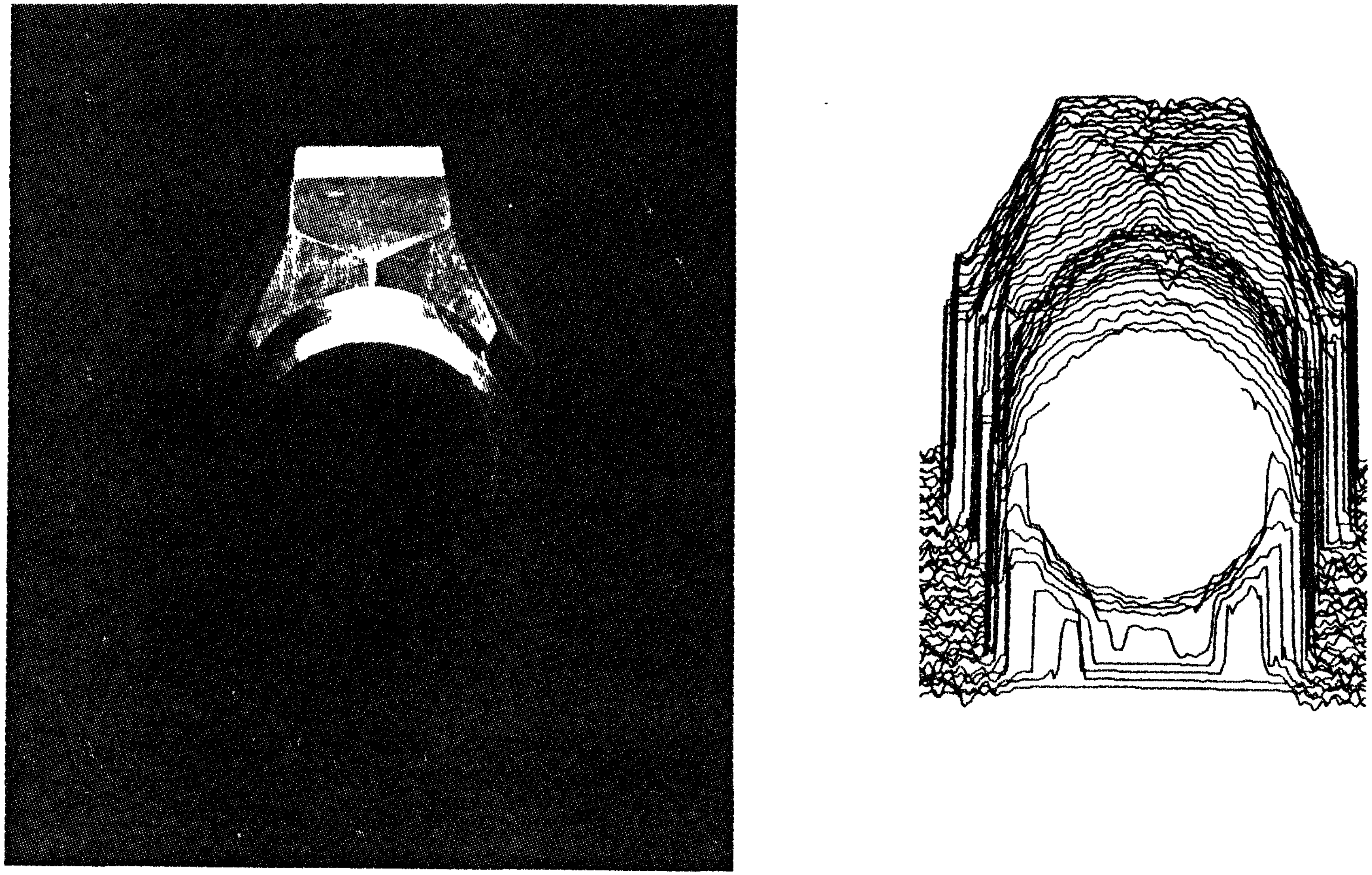

FIGURE 5. PHOTOGRAPH AND ULTRASONIC IMAGE OF A SIMULATED HANDLING SOCKET

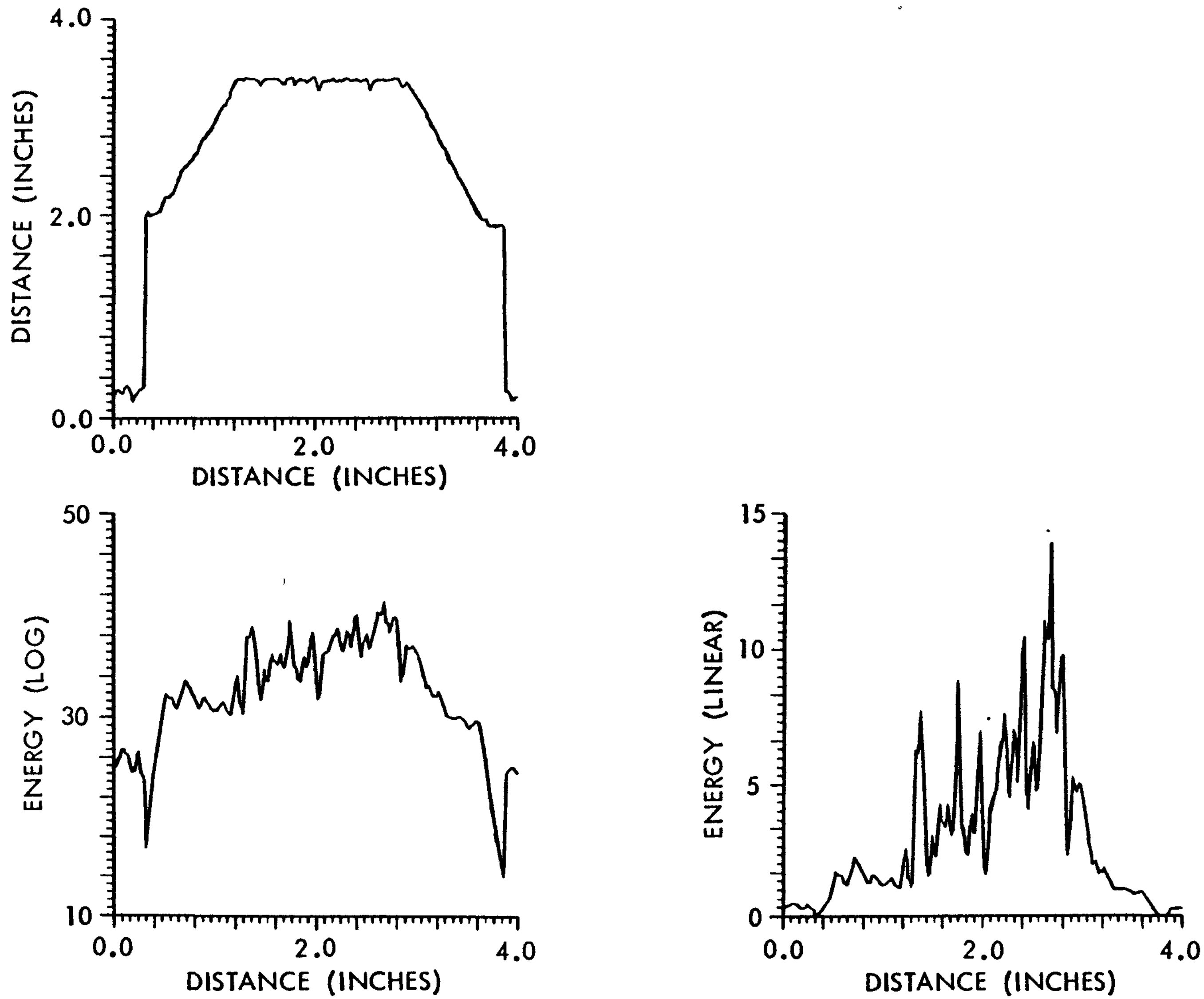

FIGURE 6. SPATIAL AND ENERGY CROSS-SECTIONS FROM THE ULTRASONIC IMAGE OF A SIMULATED HANDLING SOCKET

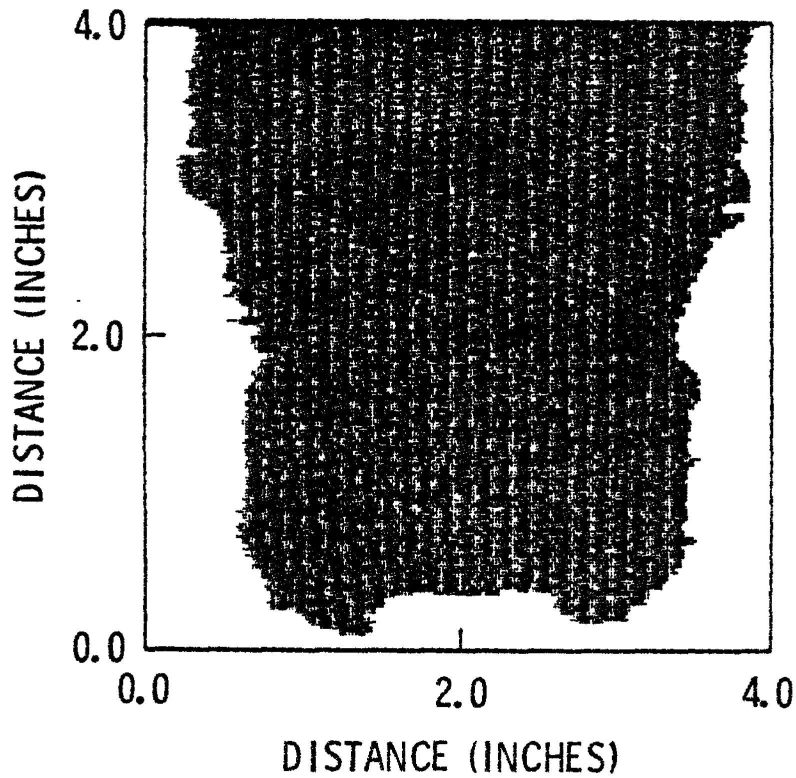

FIGURE 7. ULTRASONIC SHADOW OF THE HANDLING SOCKET ON THE SUPPORTING PLATE

V. CONCLUSIONS

The specific objective of this study was to develop algorithms and procedures for under sodium imaging of objects with off-normal surfaces. Results in a water immersion system show off-normal imaging is feasible with the following conclusions:

1. Scattered energy from off-normal surfaces varies in energy level, and this energy is not a monotonic function of inclination angle.

2. Pulse shapes of signals scattered from off-normal surfaces vary a great deal and are not at all predictable, even from smooth surfaces.

3. The centroid of received waveforms can be calculated by using an accumulated energy algorithm. The transit time corresponding to the one-half energy value gives the centroid.

4. Mapping the centroid of scattered energy waveforms from off-normal surfaces is a good algorithm for determining actual surface slopes.

5. This centroid position algorithm works well for both flat (normal and off-normal to 60°) and curved surfaces as was illustrated by imaging a simulated core component.

6. Future work is needed to decide upon the specific equipment and algorithms for final application in hot sodium.

VI. REFERENCES

1. C. K. Day, "FFTF Core and Primary Circuit Instrumentation," Proceedings of IAEA Specialist's Meeting on "The Core and Primary Circuit Instrumentation of LMFBR's," at Risley, England, January 27-29, 1976.